

Alma Mater Studiorum Università di Bologna  
Archivio istituzionale della ricerca

Gigantelline, gigantellinine and gigancrine, cherylline- and crinine-type alkaloids isolated from *Crinum jagus* with anti-acetylcholinesterase activity

This is the final peer-reviewed author's accepted manuscript (postprint) of the following publication:

*Published Version:*

Ka, S., Masi, M., Merindol, N., Di Lecce, R., Plourde, M.B., Seck, M., et al. (2020). Gigantelline, gigantellinine and gigancrine, cherylline- and crinine-type alkaloids isolated from *Crinum jagus* with anti-acetylcholinesterase activity. *PHYTOCHEMISTRY*, 175, 1-9 [10.1016/j.phytochem.2020.112390].

*Availability:*

This version is available at: <https://hdl.handle.net/11585/958200> since: 2024-06-14

*Published:*

DOI: <http://doi.org/10.1016/j.phytochem.2020.112390>

*Terms of use:*

Some rights reserved. The terms and conditions for the reuse of this version of the manuscript are specified in the publishing policy. For all terms of use and more information see the publisher's website.

This item was downloaded from IRIS Università di Bologna (<https://cris.unibo.it/>).  
When citing, please refer to the published version.

(Article begins on next page)

**Gigantelline, gigantellinine and gigancrinine, cherylline and crinine-type alkaloids isolated from *Crinum jagus* with anti-acetylcholinesterase activity**

Seydou Ka<sup>a,c</sup>, Marco Masi<sup>b</sup>, Natacha Merindol<sup>a</sup>, Roberta Di Lecce<sup>b</sup>, Mélodie B. Plourde<sup>a</sup>, Matar Seck<sup>c</sup>, Marcin Górecki<sup>d,e</sup>, Gennaro Pescitelli<sup>d</sup>, Isabel Desgagne-Penix<sup>a,\*</sup>, Antonio Evidente<sup>b,\*</sup>

<sup>a</sup>Département de Chimie, Biochimie et Physique, Université du Québec à Trois-Rivières, 3351, Boul. des Forges, C.P. 500, Trois-Rivières (Québec), G8Z 4M3, Canada

<sup>b</sup>Dipartimento di Scienze Chimiche, Università di Napoli Federico II, Complesso Universitario Monte Sant'Angelo, Via Cintia 4, 80126 Napoli, Italy

<sup>c</sup>Département de Pharmacie, Université Cheikh Anta Diop de Dakar, Dakar, Sénégal

<sup>d</sup>Dipartimento di Chimica Organica e Industriale, Via Giuseppe Moruzzi, 13, 56124 Pisa, Italy

<sup>e</sup>Institute of Organic Chemistry, Polish Academy of Sciences, ul. Kasprzaka 44/52, Warsaw 01-224, Poland

**ABSTRACT:** Three undescribed Amarylidaceae alkaloids, named gigantelline, gigantellinine and gigancrinine, were isolated from *Crinum jagus* (syn.=*Crinum giganteum*) collected in Senegal, together with the already known sanguinine, cherylline, lycorine, crinine, flexinine and the isoquinolinone derivative hippadine. Gigantelline, gigantellinine and gigancrinine were characterized as 4-(6,7-dimethoxy-2-methyl-1,2,3,4-tetrahydro-isoquinolin-4-yl)-phenol, its 7-*O*-demethyl-5'-hydroxy-4'-methoxy derivative and 5,6a,7,7a,8a,9-hexahydro-6,9a-ethano[1,3]dioxolo[4,5-*j*]oxireno[2,3-*b*]phenanthridin-9-ol, respectively, by using spectroscopic (1D and 2D  $^1\text{H}$  and  $^{13}\text{C}$  NMR and HRESIMS) and chemical methods. Their relative configuration was assigned by NOESY NMR spectra and NMR calculations, while the absolute configuration was assigned using electronic circular dichroism (ECD) experiments and calculations. Sanguinine, cherylline, crinine, flexinine, and the isoquinolinone hippadine, were isolated for the first time from *C. jagus*. Cherylline, gigantellinine, crinine, flexinine and sanguinine inhibited the activity of AChE in a dose-dependent manner, and inhibition by sanguinine was remarkably effective ( $\text{IC}_{50}=1.83 \pm 0.01 \mu\text{M}$ ). Cherylline and hippadine showed weak cytotoxicity at  $100 \mu\text{M}$ .

## 1. Introduction

Plants and microorganisms are an important reservoir of bioactive specialized metabolites. Among them, the plants of the Amaryllidaceae species are a demonstrated rich source of alkaloids and related isocarbostryl compounds, with a broad spectrum of biological activity (Evidente and Kornienko, 2009a; Nair et al., 2013a; Jin and Yao, 2019).

Amaryllidaceae plants are found in tropical and subtropical regions of the world, but essentially in Andean South America, in the Mediterranean basin, and in Southern Africa (Nair et al., 2013b). These bulbous flowering plants, including ca. 1600 species, are classified into about 75 genera (Christenhusz and Byng, 2016). Approximately one third of the known Amaryllidaceae species grow in South Africa (Nair et al., 2013b) and they are largely utilized in folk medicine (Meerow and Snijman, 1998).

The Amaryllidaceae alkaloids (AAs) are grouped into 12 ring types (Kornienko and Evidente, 2008). Many studies have been carried out on AAs since their structures provide a viable platform for phytochemicalbased drug discovery (Cimmino et al., 2017). Hundreds of structurally diverse alkaloids have been found (Kornienko and Evidente, 2008; Cimmino et al., 2017; Jin and Yao, 2019) and many have shown promising anticancer activity. Among them there are lycorine- and its related isocarbostryl narciclasine-type, crinine-type, pretazettine-type, and the montanine-type alkaloids (Cimmino et al., 2017). Galanthamine is the most promising for the treatment of the symptoms of Alzheimer's disease and it is currently being used as a cholinesterase inhibitor drug for this disease (Houghton et al., 2006). Recently, from *Narcissus tazetta* subsp. *tazetta* L., collected in Turkey, lycorine, pseudolycorine, galanthamine and 11-hydroxygalanthamine were isolated (Karakoyun et al., 2019). In addition, sarniensine, sarniesinol and crinsarnine, showing significant insecticidal activity against *Aedes aegypti*, the mosquito responsible of yellow and dengue fevers and Zika, were isolated together with several known AAs from *Nerine sarniensis* collected in South Africa (Masi et al., 2016, 2017). Coccinine,

montanine, albomaculine and incartine, belonging to the isoquinoline-, homolycorine- and lycorine-type alkaloids, were isolated from *Haemanthus humilis*, collected in the same country, with only coccinine and montanine exhibiting anticancer activity at low micromolar concentrations (Masi et al., 2019). *Crinum buphanoides*, *Crinum graminicola*, *Cyrtanthus mackenii*, *Brunsvigia grandiflora*, native species of South Africa, produced lycorine as the main alkaloid (Masi et al., 2018).

Continuing our screening on biologically active undescribed alkaloids from native and unstudied Amaryllidaceae from Africa, our interest was focused on *Crinum jagus* (syn.=*Crinum giganteum*) collected in Senegal, belonging to a genus which showed to be very rich in crinine-type alkaloids (Ghosal et al., 1985). The aqueous and organic extracts of this plant were previously investigated in different studies and showed to contain biologically active metabolites. In fact, these compounds have the potential for the treatment of inflammatory process (Kapu et al., 2001) and possesses several other important activities such as antibacterial (Adesanya et al., 1992), sedative (Amos et al., 2003), inhibition of cholinesterases (Cortes et al., 2018), antiviral (Ogbole et al., 2018) etc. However, only few reports are available on the alkaloids produced by this species (Adesanya et al., 1992; Kintsurashvili and Vachnadze, 2007; Cortes et al., 2018).

This study reports on the isolation and the chemical and biological characterization of three undescribed alkaloids, named gigantelline, gigantellinine and gigancrinine from *C. jagus*, together with five known AAs and the isoquinolinone derivative hippadine. The results of their acetylcholinesterase (AChE) inhibitory and cytotoxic activity on breast cancer cells are also discussed.

## 2. Results and Discussion

The acid organic extract of powdered bulbs of *C. jagus* was purified by a combination of column and TLC chromatography to yield three undescribed alkaloids (**1–3**, Fig. 1) together with the well-known

AAs sanguinine, cherylline, lycorine, crinine and flexinine, and the isoquinolinone hippadine (**4–9**, Fig. 1). These latter compounds were identified by comparison of their spectroscopic (essentially  $^1\text{H}$  and  $^{13}\text{C}$  NMR and ECD) and physical (specific optical rotation) data with those previously reported for **4** (Kobayashi et al., 1991), **5** (Kobayashi et al., 1984; Lebrun et al., 2003; Brossi and Teitel, 1970), **6** (Pham et al., 1998; Lamoral-Theys et al., 2009), **7** (Viladomat et al., 1995), **8** (Pham et al., 1998) and **9** (Ghosal et al., 1981; Masi et al., 2016), respectively.

The previously undescribed alkaloids **1–3**, were named gigantelline, gigantellinine and gigancrinine, respectively.

Gigantelline (**1**) has a molecular formula of  $\text{C}_{18}\text{H}_{21}\text{NO}_3$  consistent with nine hydrogen deficiencies. Its  $^1\text{H}$  and COSY spectra (Berger and Braun, 2004) (Table 1) showed the signal patterns of a tetra-substituted-tetrahydroisoquinoline and a *para*-substituted phenol ring. In particular, the singlets of two methoxy groups were observed at  $\delta$  3.83 and 3.59 while that of a N-methyl resonated at  $\delta$  2.44 (Pretsch et al., 2000). C-4 represents the carbon bridging the tetrasubstituted tetrahydroisoquinoline and the *para*-substituted phenol rings, as evidenced by the long-range couplings observed in the HMBC spectrum (Berger and Braun, 2004) (Table 1, Fig. 2). The methoxy group at  $\delta$  3.83 was located at C-6 as demonstrated by the long-range coupling with H-5 observed in the HMBC spectrum (Table 1, Fig. 2) and the coupling between MeO–C6 with both C-5 and C-6 (Table 1 and Fig. 2), while the methoxy group at  $\delta$  3.59 was positioned at C-7 as demonstrated by long range couplings observed in the same spectrum with C-7 and C-8 (Pretsch et al., 2000). These positions were confirmed by the correlations observed in the NOESY spectrum between MeO–C6 with H-5 and MeO–C7 with H-8 (Fig. 2).

The couplings observed in the HSQC spectrum (Berger and Braun, 2004) (Table 1) allowed to assign all the protonated carbons. The couplings observed in the HMBC spectrum (Table 1, Fig. 2) allowed to assign the six quaternary  $\text{sp}^2$  carbons, three of which were oxygenated (Breitmaier and

Voelter, 1987). Thus, the chemical shifts were assigned to all the protons and corresponding carbons of **1** as reported in Table 1.

These results were consistent with the bands recorded in the IR and UV spectra (Nakanishi and Solomon, 1977; Pretsch et al., 2000). According to these findings, **1** was formulated as 4-(6,7-dimethoxy-2-methyl-1,2,3,4-tetrahydro-isoquinolin-4-yl)-phenol. The structure assigned to **1** was supported by the pseudomolecular ion  $[M+H]^+$  observed in its HR ESIMS spectrum at  $m/z$  300.1591.

The structure assigned to **1** was further confirmed by the preparation of its 4'-*O*-acetyl derivative (**10**, Fig. 1) which showed the absence of the hydroxy group in the IR spectrum while its  $^1H$  NMR spectrum differed from that of **1** for the downfield shifts of H-3',5' and H-2',6' and for the singlet of the acetyl group at  $\delta$  2.29. Its ESIMS spectrum showed the pseudomolecular ion  $[M+H]^+$  at  $m/z$  342 and the fragmentation peak at  $m/z$  300  $[M+H - CH_2CO]^+$ .

Gigantellinine (**2**, Fig. 1) has a molecular formula of  $C_{18}H_{21}NO_4$  consistent with 9 hydrogen deficiencies as in **1** but differing by one extra oxygen atom. The comparison between the  $^1H$  and  $^{13}C$  NMR spectra of **1** and **2** (Table 1) showed differences essentially in the signal system of the phenol ring. In fact, this latter appears to be a 2,5-disubstituted phenol again linked through the C-1'-C-4 bond to the almost unchanged tetrahydroisoquinoline moiety, as showed by the long range couplings observed in the HMBC spectrum (Table 1, Fig. 2). Its  $^1H$  and COSY NMR spectra (Table 1) showed again two singlets due to the methoxy groups at  $\delta$  3.62 and 3.85, with the first located at C-6 in agreement with the coupling observed in the HMBC spectrum of MeO-C6 with both C-6 and C-7 (Table 1, Fig. 2). The other one was located at C-4' in agreement with the long range coupling observed between MeO-C4' and C-4'. These assignments were also confirmed by the correlations observed in the NOESY spectrum reported in Fig. 2.

Thus, **1** and **2** differed only in the position of two methoxy groups, which were assigned as reported above, and for the hydroxy groups at C-7 and C-5'. Consequently, the  $^{13}\text{C}$  NMR spectrum of **2** (Table 1) showed an extra oxygenated  $\text{sp}^2$  quaternary carbon at  $\delta$  114.9 which was assigned to carbon C-5' due to its couplings in the HMBC spectrum with H-3' (Table 1). The other  $^{13}\text{C}$  resonances remained unaltered and based on the couplings observed in the COSY, HSQC and HMBC spectra (Table 1), all the proton and carbon signals were assigned and reported in Table 1 ([Pretsch et al., 2000](#); [Breitmaier and Voelter, 1987](#)).

These findings agreed with the bands recorded in the IR and UV spectra. Thus, **2** was formulated as the 7-*O*-demethyl-5'-hydroxy-4'-methoxy derivative of **1**. Its structure was supported by the HR ESIMS spectrum which showed the pseudomolecular ion  $[\text{M}+\text{H}]^+$  at  $m/z$  316.1539.

The absolute configuration of **1** and **2** was determined by comparison of their ECD spectra with that of cherylline (**5**), as the three compounds have consistent chromophores and the same skeleton. The ECD spectra of the three alkaloids (**1**, **2** and **5**) are reported in Fig. 3 and showed a quite perfect overlapping between the spectra of cherylline and gigantellinine, while that of **1** had a mirror image appearance with respect to the former ones. Thus, as the C-4 in **5** has *S* stereochemistry ([Brossi and Teitel, 1970](#)), the same was assigned to the C-4 of **2**, while the *R* absolute configuration was assigned to the same carbon of **1**.

Thus, the same plant synthesizes two closely related alkaloids **1** and **2** with different stereochemistry at C-4. To explain this point, it is necessary to investigate the biosynthetic pathway of gigantelline and gigantellinine. Amigo Chan in his PhD thesis ([Iowa State University, 1973](#)) “Biosynthesis of cherylline using doubly-labeled norbelladine type precursor” reports some results on the biosynthesis of cherylline based on the incorporation of doubly labeled O-methyl  $[1\text{-}^3\text{H}, 1\text{-}^{14}\text{C}]$  norbelladine into *Crinum powellii*. His results confirmed the previous ones obtained by [Shaffer \(1972\)](#)



and [Miller \(1966\)](#), who already demonstrated that O-methyl [ $1'$ - $^3\text{H}$ ]norbelleadine was incorporated intact in cherylline, lycorine and ambelline. Thus, it is possible to hypothesize that gigantelline is biosynthesized from the same biosynthetic pathway and then that the intermediate cherylline is methylated at the hydroxyl group attached at C-7 by S-adenosylmethionine. Amigo Chan also postulated that montanine could be a biosynthetic precursor of a cherylline ring system but with an opposite configuration at C-4. Consequently, to clarify the origin of the different stereochemistry at C-4 in **2**, the biosynthetic pathway of gigantelline should be investigated by incorporation a suitable label (with radioactive or heavy isotopic atoms depending from the fraction of incorporation into the biosynthetic precursor) in *C. jagus*. Then the labeled gigantelline should be isolated and the site(s) of label incorporation investigated. However, this challenging project is beyond the scope of the present manuscript.

Gigancrine (**3**, Fig. 1) has a molecular formula  $\text{C}_{16}\text{H}_{17}\text{NO}_4$  with nine hydrogen deficiencies. The first investigation of its  $^1\text{H}$  and  $^{13}\text{C}$  NMR spectra (Table 2) showed that it is closely related to crinine-type alkaloids ([Ghosal et al., 1985](#); [Kornienko and Evidente, 2008](#)). These preliminary findings are consistent with the bands observed in the IR spectrum and UV spectra.

In particular, the  $^1\text{H}$  NMR and COSY spectra of **3** (Table 2) showed the expected singlets of the two protons of a 2,3,5,6-tetrasubstituted benzene ring (ring A) and the singlet of the methylene of a dioxolane ring. The two doublets of a methylene ( $\text{H}_2\text{C}$ -6) linked to the tertiary nitrogen atom account for the presence of ring B. This latter, judging also from the couplings observed in HMBC spectrum (Table 2, Fig. 2), was linked to the aromatic ring (ring A), and this latter to the dioxolane ring. Similarly, the two double doublets of  $\text{H}_2\text{C}$ -11, coupled with the multiplet and the double triplet of  $\text{H}_2\text{C}$ -12, which appeared linked to the nitrogen atom, accounted for the ethano bridge between C-10b and the nitrogen atom, which is characteristic of crinine-type alkaloids ([Ghosal et al., 1985](#); [Kornienko and Evidente,](#)

2008). In addition, the presence of ring D, joined to rings B and C, was confirmed on the basis of the couplings observed in the HMBC spectrum. The signal pattern of ring C consisted of a broad singlet (H-1) resonating at  $\delta$  4.47, which coupled with the adjacent proton (H-2), a doublet at  $\delta$  3.12 and this, in turn, with the multiplet of its adjacent proton (H-3) at  $\delta$  3.48. Both the chemical shifts of H-2 and H-3 are typical of an oxirane ring (Pretsch et al., 2000; Batterham, 1972). H-3, in turn, coupled with the protons of the adjacent methylene group (H<sub>2</sub>C-4), observed as two doublets of double doublets at  $\delta$  2.37 and 1.81, which coupled both with H-4a resonating as a double doublet at  $\delta$  3.21.

The <sup>13</sup>C NMR spectrum (Table 2) showed the signals of sixteen carbons which were all assigned by the coupling observed in the HSQC and HMBC spectra (Table 2, Fig. 2). Thus, the chemical shifts were assigned to all the protons and corresponding carbons and reported in Table 2 and gigancrinine was formulated as 5,6a,7,7a,8a,9-hexahydro-6,9a-ethano[1,3]dioxolo[4,5-j] oxireno[2,3-b]phenanthridin-9-ol (**3**). Gigancrinine then appears as a constitutional isomer of flexinine (**8**), obtained upon the shift of the hydroxy group and epoxy ring positions on ring C.

The structure assigned to **3** was supported by the data of its HR ESIMS spectrum which showed the protonated molecular ion [M+H]<sup>+</sup> at  $m/z$  288.1228.

The relative stereochemistry of **3** was deduced from the correlations observed in the NOESY spectrum (Fig. 2), from a detailed analysis of <sup>3</sup>J<sub>HH</sub> couplings and from NMR calculations. Compound **3** contains 6 different stereogenic centers (5 carbons and 1 nitrogen). However, the relative configuration of C-4a, C-10b and N is restricted by the ethano bridge, while that of C-2 and C-3 is dictated by the epoxy ring; thus, the set of possible stereoisomers is limited to 4 pairs of enantiomers. Still, the stereochemical assignment is complicated by the fact that ring C assumes a half-chair conformation, making some pieces of information not immediate. We started assuming the same configuration at C-4a, C-10b and N as for flexinine (**8**), thus with the ethano bridge in  $\beta$ -orientation (Fig. 1). The NOE

cross-peak observed between H-1 and H-2 and the small (undetectable) coupling constant suggested their *gauche* spatial relation. Furthermore, the significant cross peak between H-1 and H-10 together with the lack of cross-peaks between H-1 and H-11 allowed to assign H-1 as  $\alpha$ -oriented and the hydroxyl group attached at C-1 as  $\beta$ -oriented. The lack of coupling between H-2 and especially H-3 and H-4a in the NOESY spectrum suggested that the former hydrogens were  $\beta$ -oriented, if H-4a is  $\alpha$ -oriented as in flexinine. Finally, a set of diagnostic  $^3J_{HH}$  coupling constants was detected (Table 3). To interpret the overall set of data by means of molecular modeling, we built 4 different isomers by keeping the configuration (4a*R*,10b*S*) fixed and varying the configuration at C-1, C-2 and C-3 as (1*R*,2*R*,3*R*), (1*S*,2*R*,3*R*), (1*R*,2*S*,3*S*) and (1*S*,2*S*,3*S*). Then, we applied a computational protocol to predict  $^{13}\text{C}$  chemical shifts and  $^1\text{H}$ – $^1\text{H}$  couplings based on density functional theory (DFT) calculations (Hehre et al., 2019). The input structures were generated after a multi-step conformational search (see Computational Section) culminating in  $\omega\text{B97X-V/6-311+G(2df,2p)}/\omega\text{B97X-D/6-31G(d)}$  energy estimation and geometry optimization. Magnetic shielding and spin-spin coupling calculations were then run at  $\omega\text{B97X-D/6-31G(d)}$  and  $\omega\text{B97X-D/pcJ-0}$  level, respectively. The results for the four isomers are summarized in Table 3 and compared therein with the experiments; correlation graphs (Fig. S2) are shown in the Supporting Information. The above computational protocol normally leads to overall RMSD (root-mean-square deviations) between experimental and calculated  $^{13}\text{C}$  chemical shifts below 2 ppm (Hehre et al., 2019). In the current case, the significantly smallest RMSD of 1.8 ppm was obtained for the (1*R*,2*R*,3*R*) isomer, but an acceptable RMSD of 2.3 ppm was also obtained for the (1*R*,2*S*,3*S*) isomer. However, only the former one provided an excellent agreement between calculated and diagnostic  $^3J_{HH}$  coupling constants (Table 3). Thus, the relative configuration 1*R*\*,2*R*\*,3*R*\*,4a*R*\*,10b*S*\* was assigned to **3**.

The absolute configuration of **3** was inferred by its ECD spectrum (Fig. 4), which was very similar to that of flexinine (**8**), either reported in the literature (Pham et al., 1998) or measured on our sample of **8**. The ECD spectra of gigantocrinine (**3**), crinine (**7**), flexinine (**8**) and related alkaloids are mainly determined by the configuration of the chirality centers on ring B, which is close to the aromatic chromophore (Wagner et al., 1996; Pham et al., 1998). Therefore, we anticipated the configuration of **3** and **8** to be the same as for the corresponding chirality centers C-4a and C-10b. The final confirmation came from the comparison between the experimental ECD spectrum of **3** with that calculated by time-dependent DFT (TD-DFT) (Superchi et al., 2018; Pescitelli and Bruhn, 2016). Using input structures with (1*R*,2*R*,3*R*,4*aR*,10*bS*) configuration, the spectrum calculated at B3LYP/def2-TZVP/PCM level (solvent model for acetonitrile) fitted very well the experimental spectrum (Fig. 4). Therefore, the absolute configuration of gigantocrinine was ultimately assigned as (1*R*,2*R*,3*R*,4*aR*,10*bS*)-**3**.

Few references are available on the alkaloids produced by *C. jagus* isolated in different parts of the world (Adesanya et al., 1992; Kintsurashvili and Vachnadze, 2007; Cortes et al., 2018) but its aqueous and organic extracts showed several biological activities (Kapu et al., 2001; Adesanya et al., 1992; Amos et al., 2003; Cortes et al., 2018; Ogbole et al., 2018). Among them one the most promising resulted to be the inhibition of acetylcholinesterase (AChE) (Houghton et al., 2004; Cortes et al., 2018).

AChE is a serine protease located at neuromuscular junctions, in cholinergic synapses of the central nervous system (Brimijoin, 1983) and in red blood cells (Heller and Hanahan, 1972; Szelenyi et al., 1982). Currently, AChE inhibitors have become the main target treatment for Alzheimer's disease and donepezil, rivastigmine, and galantamine are the major therapies approved for its treatment (Lahiri et al., 2002). However, these drugs are not curatives, their benefit are short-term (Giacobini, 2000), and cause serious side effects (Moodie et al., 2019). Therefore, the discovery of new drugs for Alzheimer's disease with improved AChE inhibition and less side effects is required (Kim et al., 2017).

All isolated compounds, except for hippadine that was not obtained in sufficient amount, were assayed for their AChE inhibitory activity. Galanthamine hydrobromide was used as a positive control. Cherylline (**5**), gigantellinine (**2**), crinine (**7**), flexinine (**8**) and sanguinine (**4**) all inhibited the activity of AChE in a dose-dependent manner (Table 4, Fig. S3) whereas gigantelline (**1**), lycorine (**6**) and gigancrine (**3**) did not. The results obtained testing lycorine are in perfect agreement with the data previously reported ([Elgorashi et al., 2004](#); [Ortiz et al., 2018](#)).

Cherylline is a 4-arylisoquinoline derivative, a compound with a weak AChE inhibitory activity ([Bastida et al., 2006](#)). Therefore, the low AChE inhibitory activity observed for gigantelline is not surprising. Gigantellinine is less active than cherylline, according to our study probably for its opposite stereochemistry at C-4. Flexinine, tested for the first time, and crinine had weak AChE inhibitory activities. The results of crinine are in agreement with the data previously reported ([Elgorashi et al., 2004](#)). The most active AA in the AChE inhibition assay was sanguinine (**4**), a galantamine-type alkaloid, with an  $IC_{50}$  value of  $1.83 \pm 0.01 \mu M$  and was 4 times more active than our positive control galantamine ( $IC_{50}$  of  $7.2 \mu M$ ; Fig. S3). This results are consistent with those recently reported by [Ortiz et al. \(2018\)](#) and with the similarity between the two alkaloids sturture that differs only in the substituents on the benzene ring. Concerning the AAs belonging to crinine group (**3**, **7** and **8**), the results showed that the stereochemistry of the ethano bridge is not important for the activity while the substitution of C ring plays an important role.

Cytotoxic activity was measured on human breast cancer cell line MCF-7 using the XTT cell viability assay. Lycorine was used as a positive control and it was toxic at all concentrations tested (Fig. S4). Sanguinine, flexinine, gigancrine and crinine did not exhibit any detectable cytotoxic activity on MCF-7 cells. Cherylline, hippadine, gigantelline, gigantellinine and sanguinine had a significant cytotoxicity at  $400 \mu M$  (Fig. S5). At  $100 \mu M$ , only hippadine and cherylline remained weakly but

significantly cytotoxic, whereas all compounds lost any cytotoxic potential at lower concentrations (Fig. S4). This is in agreement with the strong anticancer activity showed by the isocarbostryl narciclasine close to lycorine ([Cimmino et al., 2017](#)).

Thus, the undescribed compounds are not good candidate as antibreast cancer drugs. However, other cell lines derived from different cancer types could be tested in the future. Further bioassays measuring other biological activities such as larvicidal, antimicrobial and anti-inflammatory will also be investigated in future studies.

### 3. Conclusions

In conclusion, eight Amaryllidaceae alkaloids and an isoquinolinone derivative were isolated from *C. jagus* collected in Senegal. Five alkaloids resulted to be known and identified as sanguinine, cherylline, lycorine, crinine and flexinine, while the isoquinolinone derivative was identified as hippadine. The other three resulted to be previously undescribed tetrahydroisoquinoline- and crinine-type alkaloids and were named gigantelline, gigantellinine and gigancrine. Alkaloids belonging to tetrahydroisoquinoline subgroup are rarely isolated from Ammaryllidaceae plants. To the best of our knowledge this is the first report of alkaloids produced by *C. jagus* collected in Senegal with sanguinine, cherylline, crinine, flexinine, and isoquinolinone hippadine isolated for the first time from this species. The isolated compounds were evaluated for their acetylcholinesterase (AChE) inhibitory potential and cytotoxic activity on the breast cancer cell line MCF-7. Cherylline, gigantellinine, crinine, flexinine and sanguinine inhibited the activity of AChE in a dose-dependent manner and sanguinine inhibition was remarkably effective. Cherylline and hippadine showed a weak cytotoxicity potential at 100  $\mu$ M. This study can expand the chemical library of Amaryllidaceae alkaloids and their possible application in medicine.

## 4. Experimental

### 4.1. General Experimental Procedures

A Perkin-Elmer Spectrum 100 Fourier transform infrared (FTIR) spectrometer was employed to record infrared (IR) spectra on a glassy film. UV spectra were measured in CH<sub>3</sub>OH on a JASCO V-530 spectrophotometer. ECD spectra of **1**, **2**, **4**, **5**, **7** and **8** were recorded on a JASCO J-815 spectrometer in CH<sub>3</sub>OH (c 0.3). The ECD spectra of **3** were recorded with a JASCO J-715 spectropolarimeter, on CH<sub>3</sub>CN solutions and using a quartz cell with 0.01 cm path-length. ECD measurement parameters were the following: scan speed 100 nm/min; time-constant 0.5 s; bandwidth 1 nm; 4 accumulations. <sup>1</sup>H and <sup>13</sup>C NMR spectra were recorded at 500/125 MHz in CD<sub>3</sub>OD on Varian spectrometers. The same solvent was used as internal standard. Carbon multiplicities were determined by DEPT spectra (Berger and Braun, 2004) DEPT, COSY-45, HSQC, HMBC (Berger and Braun, 2004), were performed using Varian microprograms. HRESI mass spectra and liquid chromatography (LC)/MS analyses were performed using the LC/MS TOF system AGILENT 6230B, HPLC 1260 Infinity. The HPLC separations were performed with a Phenomenex LUNA (C18 (2) 5u 150×4.6 mm). The ESI MS/MS were recorded on Alliance waters 2695 HPLC-MS/MS QQQ. Analytical and preparative TLC were performed on silica gel (Kieselgel 60, F<sub>254</sub>, 0.25 and 0.5mm respectively, Merck) plates. The spots were visualized by exposure to UV radiation (253), or iodine vapour. Column chromatography (CC) was performed using silica gel (Kieselgel 60, 0.063–0.200 mm, Merck).

### 4.2. Plant material

Bulbs of *Crinum jagus* (syn.=*Crinum giganteum*) were collected in Senegal, in Montrolland district (14°55'56,22''N and 16°59'38,62''W), in December 2018 (Fig. S1). A senior scientist from the

Herbarium of IFAN of University Cheikh Anta Diop of Dakar taxonomically identified the plant materials.

#### 4.3. Extraction and purification

Fresh bulbs of *C. jagus* were dried at room temperature and then finely powdered. The resultant powder (1.35 kg) was extracted with 1% H<sub>2</sub>SO<sub>4</sub>, (2 x 2L) overnight at room temperature. The suspension was filtered through cloth and successively centrifuged at 10 °C at 7000 rpm for 30 min. The acid extract was alkalized to pH 9–10 with 12 N NaOH. The aqueous solution was extracted with EtOAc (3 x 1.2 L), and the organic extracts were combined, dried (Na<sub>2</sub>SO<sub>4</sub>) and evaporated under reduced pressure to give a brown oil residue (3.0 g). This latter was crystallized by EtOH obtaining lycorine (**6**, 600 mg) as white crystals. The mother liquors of crystallization were dried and the residue (2.4 g) was fractionated by column chromatography eluted with CHCl<sub>3</sub>-EtOAc-MeOH (2:2:1), affording eighteen groups of homogeneous fractions (F1–F18). The residue (134.8 mg) of fraction F2 was purified on silica gel chromatography and eluted with CHCl<sub>3</sub>-*i*-PrOH (95:5), yielding eleven fractions. The residue (10.5 mg) of fraction 2 was further purified on preparative TLC and eluted with CHCl<sub>3</sub>, yielding hippadine (**9**, 1.6 mg) as an amorphous solid. The residues (90.5 and 128.2 mg) of fractions F7 and F8 were combined and treated with hot EtOH, affording a homogeneous amorphous precipitate which being an undescribed compound, as below reported, was named gigantelline (**1**, 50.7 mg, R<sub>f</sub> 0.55 in CHCl<sub>3</sub>-EtOAc-MeOH (2:2:1)). The supernatant was purified by column chromatography, eluted with CHCl<sub>3</sub>-CH<sub>3</sub>OH (85:15) obtaining, cherylline (**5**, 15.4 mg) and an amorphous solid, which being undescribed as below reported, was named gigantellinine (**2**, 17.72 mg, R<sub>f</sub> 0.43) and further amount of gigantelline (20.8 mg for a total of 71.5 mg). The residue (98.5 mg) of fraction F17 of the initial column was purified on silica gel chromatography and eluted with CHCl<sub>3</sub>-CH<sub>3</sub>OH (8:2), yielding 6 fractions. The residue (27.5 mg) of



fraction 2 was further purified by preparative TLC eluted with  $\text{CHCl}_3$ – $\text{CH}_3\text{OH}$  (85:15), yielding flexinine (**8**, 16.0 mg), as crystals. The residue (230.6 mg) of fraction F18 of the initial column was purified by silica gel column, eluted with  $\text{EtOAc}$ – $\text{CH}_3\text{OH}$ – $\text{H}_2\text{O}$  (75:15:10), yielding 8 fractions. The residue of fraction 6 was an amorphous solid which was identified, as below reported, as crinine (**7**, 42.3 mg). The residue of fraction 8 was identified as sanguinine (**4**, 6.7 mg). The residue (23.9 mg) of fraction 4 was further purified on preparative TLC and eluted with  $\text{CH}_2\text{Cl}_2$ – $\text{CH}_3\text{OH}$  (75:25), yielding an amorphous solid which being an undescribed compound, as below reported, was named gigancrine (**3**, 5.5 mg,  $R_f$  0.55).

*Gigantelline (1)*.  $[\alpha]_D^{25} +16.3$  (c 2.9,  $\text{CH}_3\text{OH}$ ); UV  $\lambda_{\text{max}}$  nm (log  $\epsilon$ ) 281 (3.35); IR  $\nu_{\text{max}}$  3291, 1588, 1512, 1465  $\text{cm}^{-1}$ ;  $^1\text{H}$  and  $^{13}\text{C}$  NMR, see Table 1; HR ESIMS (+)  $m/z$ : 300.1591  $[\text{M} + \text{H}]^+$  (calculated for  $\text{C}_{18}\text{H}_{22}\text{NO}_3$  300.1600).

*Gigantellinine (2)*.  $[\alpha]_D^{25} -39.1$  (c 0.8,  $\text{CH}_3\text{OH}$ ); UV  $\lambda_{\text{max}}$  nm (log  $\epsilon$ ) 283 (3.64); IR  $\nu_{\text{max}}$  3390, 1588, 1506, 1462  $\text{cm}^{-1}$ ;  $^1\text{H}$  and  $^{13}\text{C}$  NMR, see Table 1; HR ESIMS (+)  $m/z$ : 316.1539  $[\text{M} + \text{H}]^+$  (calculated for  $\text{C}_{18}\text{H}_{22}\text{NO}_4$  316.1549).

*Gigancrine (3)*.  $[\alpha]_D^{25} -4.5$  (c 0.3,  $\text{CH}_3\text{OH}$ ); UV  $\lambda_{\text{max}}$  nm (log  $\epsilon$ ) 294 (2.59); IR  $\nu_{\text{max}}$  3456, 1505, 1487, 1288  $\text{cm}^{-1}$ ;  $^1\text{H}$  and  $^{13}\text{C}$  NMR, see Table 2; HR ESIMS (+)  $m/z$ : 288.1228  $[\text{M} + \text{H}]^+$  (calculated for  $\text{C}_{16}\text{H}_{18}\text{NO}_4$  288.1236).

*Sanguinine (4)*.  $[\alpha]_D^{25} -100.4$  (c 0.6,  $\text{EtOH}$ ) [[Kobayashi et al., 1991](#):  $[\alpha]_D^{25} -133.0$  (c 0.2,  $\text{EtOH}$ )];  $^1\text{H}$  and  $^{13}\text{C}$  NMR spectra are identical to those previously reported ([Kobayashi et al., 1991](#)); ESIMS (+)  $m/z$ : 274  $[\text{M} + \text{H}]^+$ .

*Cherylline (5)*.  $[\alpha]_D^{25} -68.4$  (c 0.1,  $\text{CH}_3\text{OH}$ ) [[Kobayashi et al., 1984](#):  $[\alpha]_D^{25} -70.6$  (c 0.2,  $\text{CH}_3\text{OH}$ )];  $^1\text{H}$  and  $^{13}\text{C}$  NMR spectra are identical to those previously reported ([Kobayashi et al., 1984](#); [Lebrun et al., 2003](#)) as well ECD ([Brossi and Teitel, 1970](#)); ESIMS (+)  $m/z$ : 286  $[\text{M} + \text{H}]^+$ .

*Lycorine (6)*.  $[\alpha]_D^{25}$  -72.5 (c 0.1, CH<sub>3</sub>OH) [Pham et al., 1998:  $[\alpha]_D^{25}$  -71.2 (c 0.1, CH<sub>3</sub>OH)]; <sup>1</sup>H and <sup>13</sup>C NMR spectra are identical to those previously reported (Lamoral-Theys et al., 2009). ESIMS (+) *m/z*: 288 [M + H]<sup>+</sup>.

*Crinine (7)*.  $[\alpha]_D^{25}$  -17.9 (c 0.6, EtOH) [Viladomat et al., 1995:  $[\alpha]_D^{22}$  -9.0 (c 0.6, EtOH)]; <sup>1</sup>H and <sup>13</sup>C NMR and specific optical rotation are identical to those previously reported (Viladomat et al., 1995). ESIMS (+) *m/z*: 272 [M + H]<sup>+</sup>.

*Flexinine (8)*.  $[\alpha]_D^{25}$  -12.7 (c 0.1, CH<sub>3</sub>OH) [Pham et al., 1998:  $[\alpha]_D^{25}$  -12.5 (c 0.1, CH<sub>3</sub>OH)]; <sup>1</sup>H and <sup>13</sup>C NMR and specific optical rotation are identical to those previously reported (Pham et al., 1998). ESIMS (+) *m/z*: 288 [M + H]<sup>+</sup>.

*Hippadine (9)*. <sup>1</sup>H and <sup>13</sup>C NMR are identical to those previously reported (Ghosal et al., 1981; Masi et al., 2016); ESIMS (+) *m/z*: 812 [3M + Na]<sup>+</sup>, 549 [2M + Na]<sup>+</sup>, 286 [M + Na]<sup>+</sup> and 264 [M + H]<sup>+</sup>.

*4'-O-Acetylgigantelline (10)*. Gigantelline (**1**, 2.0 mg), was acetylated used a common method to obtain the corresponding acetyl derivative **10** as an amorphous solid (1.46 mg). **10** had: UV  $\lambda_{\max}$  (log  $\epsilon$ ) 285 (3.15) nm; IR  $\nu_{\max}$  1763, 1607, 1512, 1459, 1217 cm<sup>-1</sup>; <sup>1</sup>H NMR, differed from that of **1** only for the following signals:  $\delta$ , 7.23 (2H, d, *J*=8.6 Hz, H-3' and H-5'), 7.07 (2H, d, *J* = 8.6 Hz, H-2' and H-6'), 2.29 (3H, s, OAc); ESIMS (+) *m/z*: 342 [M + H]<sup>+</sup> and 300 [M + H - CH<sub>2</sub>CO]<sup>+</sup>.

#### 4.4. Computational methods

Molecular mechanics, Hartree-Fock (HF) and density functional theory (DFT) calculations were run with Spartan'18 (Wavefunction, Inc., Irvine CA, 2018), with standard parameters and convergence criteria. DFT and time-dependent (TD) DFT calculations were run with Gaussian16 (Frisch et al., 2016) with default grids and convergence criteria. NMR calculations were run on four isomers of **3** with the configurations (1*R*,2*R*,3*R*,4*aR*,10*bS*), (1*S*,2*R*,3*R*,4*aR*,10*bS*), (1*R*,2*S*,3*S*,4*aR*,10*bS*) and

(1*S*,2*S*,3*S*,4*aR*,10*bS*). The conformers obtained by a conformational search run with the Monte Carlo algorithm using Merck molecular force field (MMFF) were geometry-optimized at HF/3-21G level, screened by single-point calculations at  $\omega$ B97X-D/6-31G(d) level, and geometry-optimized at the same level. Final energies and populations were estimated at the  $\omega$ B97X-V/6-311+G(2df,2p) level, according to the procedure described by [Hehre et al., \(2019\)](#). The procedure afforded up to 3 energy minima for each isomer.  $^{13}\text{C}$ -NMR chemical shifts were then calculated with the GIAO method at  $\omega$ B97XD/6-31G(d) level; an empirical correction was applied depending on the number of bonds to the carbon and on the bond lengths ([Hehre et al., 2019](#)).  $^1\text{H}$ - $^1\text{H}$  NMR spin-spin coupling constants were calculated at  $\omega$ B97X-D/pcJ-0 level, including only the Fermi contact (FC) term. ECD calculations were run on the (1*R*,2*R*,3*R*,4*aR*,10*bS*)-**3** isomer. The sets of low-energy minima found as described above were re-optimized at the  $\omega$ B97X-D/6-311+G(d,p)/PCM level including the IEF-PCM continuum solvent model for acetonitrile. TDDFT calculations were run at the B3LYP/def2-TZVP/PCM and CAM-B3LYP/def2-TZVP/PCM levels, yielding consistent results. They included 32 excited states (roots) in each case. Average ECD spectra were computed by weighting component ECD spectra with Boltzmann factors at 300 K estimated from DFT internal energies, and were plotted using the program SpecDis ([Bruhn et al., 2017](#)), using dipole-length rotational strengths; the difference with dipole-velocity values was negligible in all cases.

#### 4.5. Cell culture

The human breast cancer cell line MCF-7 was kindly provided by the Celine Van Themsche and Carlos Reyes-Moreno laboratory's at the Université du Québec in Trois-Rivières (Trois-Rivières, Canada). Cells were grown in complete Dulbecco's modified Eagle medium (DMEM, Wisent) with 10% fetal bovine serum (FBS) and antibiotics (100  $\mu\text{g/mL}$  penicillin and 100  $\mu\text{g/mL}$  streptomycin and

plasmocin, (Invivogen Cedar Lane, Burlington, Ontario, Canada). Cells were maintained in a humidified atmosphere at 37 °C and 5% CO<sub>2</sub>.

#### 4.6. XTT cell viability assay

Cytotoxicity properties were evaluated using the XTT assay kit (Roche, [sigma-aldrich.com](http://sigma-aldrich.com)). MCF-7 were seeded at  $10 \times 10^3$  cells per well in 96-well plates and cultured for 24 h. Then, they were treated with the compounds at concentrations ranging from 0.4 to 400  $\mu$ M for 72 h. At that time, media was replaced by fresh phenol-free DMEM medium (Wisent) containing 0.3 mg/mL XTT. After 4 h of incubation, the absorbance was measured at 450 nm using a microplate spectrophotometer (Synergy H1, Biotek, Québec, Canada). Experiments were performed in triplicate. Control assays were performed in the presence of compounds and in the absence of cells, as well as in the presence of cells and in the absence of compounds (with 0.1% DMSO) and were used to assess maximal cytotoxicity. The percentage of cells viability was calculated at each concentration for each compound.

#### 4.7. *In vitro* Acetylcholinesterase (AChE) activity assay

*In vitro* AChE activity was assessed according to Ellman's colorimetric method ([Ellman et al., 1961](#)), with some modifications using the Acetylcholinesterase Assay Kit (Abcam). Compounds were dissolved in DMSO at 100 mM. Galanthamine hydroxybromide (Tocris Bioscience, Bristol, UK, 2016) dissolved in H<sub>2</sub>O at 50mM was used as standard compound. Samples were diluted in Assay Buffer to a final concentration ranging from 0.001 to 1000  $\mu$ M. The AChE stock solution was prepared by resuspension in 0.1% bovine serum albumin/double distilled (dd) H<sub>2</sub>O at 50 U/mL first and then dissolved in Assay Buffer at 0.25 U/mL, right before the assay. The substrates acetylthiocholine iodide and 5,5'-dithiobis-2-nitrobenzoic acid (DTNB) were dissolved in ddH<sub>2</sub>O and assay buffer, respectively. For the enzymatic

reaction in 96-well plates, samples (50  $\mu$ L) were mixed with AChE solution (45  $\mu$ L) and the reaction was started by the addition of 5  $\mu$ L of Ellman's mixture (acetylthiocholine and DNTB). Following an incubation of 5 min at room temperature, the absorbance was measured at 412 nm using a microplate spectrophotometer every 2 min for 10 min (Synergy H1, Biotek, Québec, Canada). Negative control was performed in the absence of enzyme, whereas positive control was assayed in the absence of compound (with 0.1% DMSO). All experiments were performed in triplicates, and the percentage of anti-AChE activity was calculated according to the following formula:  $((E - S)/E) \times 100$ , where E is the activity of enzyme without test sample and S is the activity of the enzyme with the test sample.

#### *4.8. Statistical analysis*

Results are presented as bar plots or curves with dots showing the mean with error bars  $\pm$  standard deviation of the mean. Statistical analyses were performed using the GraphPad Prism 8 software. The means of 2 variables (e.g. inhibition or cytotoxicity and concentration) were compared between groups using a two-way ANOVA with Dunnet's multiple comparisons test. Results were considered significant when the  $p$ -value ( $p$ )  $< 0.05$ .

#### **Acknowledgments**

The authors would like to thank professors C  line Van Themsche and Carlos Reyes-Moreno and Maria-Grazia Martinoli (Universit   du Qu  bec in Trois-Rivi  res, Canada) for kindly providing MCF-7 cells and cell cultures equipment. This work was supported by the Centre SEVE international scholarship to S.K. and by the Natural Sciences and Engineering Research Council of Canada (NSERC) award number RGPIN 05294-2014 (Discovery) to I.D-P. A.E. is associated to the Instituto di Chimica

Biomolecolare del CNR, Pozzuoli, Italy. M.G. thanks the program Bekker of the Polish National Agency for Academic

Exchange. G.P. acknowledges the CINECA award under the ISCRA initiative for the availability of high-performance computing resources and support.

## Appendix A. Supplementary data

Supplementary data to this article can be found online at <https://doi.org/10.1016/j.phytochem.2020.112390>.

## References

- Adesanya, S.A., Olugbade, T.A., Odebiyi, O.O., Aladesanmi, J.A., 1992. Antibacterial alkaloids in *Crinum jagus*. *Int. J. Pharmacogn.* 30, 303–307.
- Amos, S., Binda, L., Akah, P., Wambebe, C., Gamaniel, K., 2003. Central inhibitory activity of the aqueous extract of *Crinum giganteum*. *Fitoterapia* 74, 23–28.
- Bastida, J., Lavilla, R., Viladomat, F., 2006. Chemical and biological aspects of Narcissus alkaloids. *Alkaloids - Chem. Biol.* 63, 87–179.
- Batterham, T.J., 1972. *NMR Spectra of Simple Heterocycles*. Wiley, New York, pp. 365.
- Berger, S., Braun, S., 2004. *200 and More Basic NMR Experiments: a Practical Course*. Wiley-VCH, Weinheim.
- Breitmaier, E., Voelter, W., 1987. *Carbon-13 NMR Spectroscopy*. VCH, Weinheim, pp. 183–280.
- Brimijoin, S., 1983. Molecular forms of acetylcholinesterase in brain, nerve and muscle: nature, localization and dynamics. *Prog. Neurobiol.* 21, 291–322.
- Brossi, A., Teitel, S., 1970. Synthesis of cherylline. *J. Org. Chem.* 35, 3559–3561.

- Bruhn, T., Schaumlöffel, A., Hemberger, Y., Pescitelli, G., 2017. SpecDis Version 1.70. Berlin, Germany. <https://specdis-software.jimdo.com/>.
- Christenhusz, M.J., Byng, J.W., 2016. The number of known plants species in the world and its annual increase. *Phytotaxa* 26, 201–217.
- Cimmino, A., Masi, M., Evidente, M., Superchi, S., Evidente, A., 2017. Amaryllidaceae alkaloids: absolute configuration and biological activity. *Chirality* 29, 486–499.
- Cortes, N., Sierra, K., Alzate, F., Osorio, E.H., Osorio, E., 2018. Alkaloids of Amaryllidaceae as inhibitors of Cholinesterases (AChEs and BChEs): an integrated bioguided study. *Phytochem. Anal.* 29 (2), 217–227.
- Elgorashi, E.E., Stafford, G.I., van Staden, J., 2004. Acetylcholinesterase enzyme inhibitory effects of Amaryllidaceae alkaloids. *Planta Med.* 70, 260–262.
- Ellman, G.L., Courtney, K.D., Andres Jr., V., Featherstone, R.M., 1961. A new and rapid colorimetric determination of acetylcholinesterase activity. *Biochem. Pharmacol.* 7, 88–95.
- Evidente, A., Kornienko, A., 2009. Anticancer evaluation of structurally diverse Amaryllidaceae alkaloids and their synthetic derivatives. *Phytochemistry Rev.* 8, 449–459.
- Frisch, M.J., Trucks, G.W., Schlegel, H.B., et al., 2016. Gaussian 16, Revision A.03. Gaussian, Inc., Wallingford CT.
- Ghosal, S., Rao, P.H., Jaiswal, D.K., Kumar, Y., Frahm, A.W., 1981. Alkaloids of *Crinum pratense*. *Phytochemistry* 20, 2003–2007.
- Ghosal, S., Saini, K.S., Razdan, S., 1985. *Crinum* alkaloids: their chemistry and biology. *Phytochemistry* 24, 2141–2156.
- Giacobini, E., 2000. Cholinesterase inhibitors stabilize Alzheimer's disease. *Ann. N. Y. Acad. Sci.* 920, 321–327.

- Hehre, W., Klunzinger, P., Deppmeier, B., Driessen, A., Uchida, N., Hashimoto, M., Fukushi, E., Takata, Y., 2019. Efficient protocol for accurately calculating  $^{13}\text{C}$  chemical shifts of conformationally flexible natural products: scope, assessment, and limitations. *J. Nat. Prod.* 82, 2299–2306.
- Heller, M., Hanahan, D.J., 1972. Human erythrocyte membrane bound enzyme acetylcholinesterase. *Biochim. Biophys. Acta* 255, 251–272.
- Houghton, P.J., Agbedahunsi, J.M., Adegbulugbe, A., 2004. Choline esterase inhibitory properties of alkaloids from two Nigerian *Crinum* species. *Phytochemistry* 65, 2893–2896.
- Houghton, P.J., Ren, Y., Howes, M.J., 2006. Acetylcholinesterase inhibitors from plants and fungi. *Nat. Prod. Rep.* 23, 181–199.
- Jin, Z., Yao, G., 2019. Amaryllidaceae and *Sceletium* alkaloids. *Nat. Prod. Rep.* 36, 1462–1488.
- Kapu, S.D., Ngwai, Y.B., Kayode, O., Akah, P.A., Wambebe, C., Gamaniel, K., 2001. Antiinflammatory, analgesic and anti-lymphocytic activities of the aqueous extract of *Crinum giganteum*. *J. Ethnopharmacol.* 78, 7–13.
- Karakoyun, G., Masi, M., Cimmino, A., Önü, M.A., Somer, N.U., Kornienko, K., Evidente, A., 2019. A brief up-to-date overview of Amaryllidaceae alkaloids: phytochemical studies of *Narcissus tazetta* subsp. *tazetta* L., collected in Turkey. *Nat. Prod. Comm.* <https://doi.org/10.1177/1934578X19872906>.
- Kim, Y., Lim, H.S., Kim, Y., Lee, J., Kim, B.Y., Jeong, S.J., 2017. Phytochemical quantification and the in vitro acetylcholinesterase inhibitory activity of *Phellodendron chinense* and its components. *Molecules* 22, 925.
- Kintsurashvili, L., Vachnadze, V., 2007. Plants of the Amaryllidaceae family grown and introduced in Georgia: a source of galanthamine. *Pharm. Chem. J.* 41, 492–494.



- Kobayashi, S., Tokumoto, T., Kihara, M., Imakura, Y., Shingu, T., Taira, Z., 1984. Alkaloidal constituents of *Crinum latifolium* and *Crinum bulbispermum* (Amaryllidaceae). Chem. Pharm. Bull. 32, 3015–3022.
- Kobayashi, S., Satoh, K., Numata, A., Shingu, T., Kihara, M., 1991. Alkaloid N-oxides from *Lycoris sanguinea*. Phytochemistry 30, 675–677.
- Kornienko, A., Evidente, A., 2008. Chemistry, biology, and medicinal potential of narciclasine and its congeners. Chem. Rev. 108, 1982–2014.
- Lahiri, D.K., Farlow, M.R., Greig, N.H., Sambamurti, K., 2002. Current drug targets for Alzheimer's disease treatment. Drug Dev. Res. 56, 267–281.
- Lamoral-Theys, D., Andolfi, A., Van Goietsenoven, G., Cimmino, A., Le Calvé, B., Wauthoz, N., Mégalizzi, V., Gras, T., Bruyère, C., Dubois, J., Mathieu, V., Kornienko, A., Kiss, R., Evidente, A., 2009. Lycorine, the main phenanthridine Amaryllidaceae alkaloid, exhibits significant antitumor activity in cancer cells that display resistance to proapoptotic stimuli: an investigation of structure-activity relationship and mechanistic insight. J. Med. Chem. 52, 6244–6256.
- Lebrun, S., Couture, A., Deniau, E., Grandclaudeon, P., 2003. A new synthesis of (+)-and (–)-cherylline. Org. Biomol. Chem. 1, 1701–1706.
- Lee Amigo Chan, J., 1973. Biosynthesis of Cherylline Using a Doubly Labeled Norbelladine-type Precursors. Ph.D. Thesis, Library, Iowa State University of Science and Technology, Ames, Iowa, USA. <https://pdfs.semanticscholar.org/43d0/33a4959c32277cc69f541993406268387b45.pdf> Last consulted 29/03/2020.
- Masi, M., Cala, A., Tabanca, N., Cimmino, A., Green, I., Bloomquist, J., van Otterlo, W., Macias, F., Evidente, A., 2016. Alkaloids with activity against the Zika virus vector *Aedes aegypti* (L.)

crinsarnine and sarniensinol, two new crinine and mesembrine type alkaloids isolated from the South African plant *Nerine sarniensis*. *Molecules* 21, 1432.

- Masi, M., van der Westhuyzen, A.E., Tabanca, N., Evidente, M., Cimmino, A., Green, I.R., Bernier, U.R., Becnel, J.J., Bloomquist, J.R., van Otterlo, W.A., Evidente, A., 2017. Sarniensine, a mesembrine-type alkaloid isolated from *Nerine sarniensis*, an indigenous South African Amaryllidaceae, with larvicidal and adulticidal activities against *Aedes aegypti*. *Fitoterapia* 116, 34–38.
- Masi, M., Mubaiwa, B., Mabank, T., Karakoyun, Ç., Cimmino, A., Van Otterlo, W.A.L., Green, I.R., Evidente, A., 2018. Alkaloids isolated from indigenous South African Amaryllidaceae: *Crinum buphanoides* (welw. Ex baker), *Crinum graminicola* (I. Verd.), *Cyrtanthus mackenii*. *S. Afr. J. Bot.* 118, 188–191.
- Masi, M., Gunawardana, S., van Rensburg, M.J., James, P.C., Mochel, J.G., Heliso, P.S., Albalawi, A.S., Cimmino, A., van Otterlo, W.A.L., Kornienko, A., Green, I.R., Evidente, A., 2019. Alkaloids isolated from *Haemanthus humilis* Jacq., an indigenous South African Amaryllidaceae: anticancer activity of coccinine and montanine. *South Afr. J. Bot.* 126, 277–281.
- Meerow, A.W., Snijman, D.A., 1998. Amaryllidaceae. In: Kubitzki, K. (Ed.), *The Families and Genera of Vascular Plants*. vol. 3. Springer, Berlin, pp. 83–110.
- Miller, J.A., 1966. Biosynthetic Studies on Tazettine and Ambelline. Ph.D. Thesis, Library, Iowa State University of Science and Technology, Ames, Iowa, USA.
- Moodie, L.W., Sepčić, K., Turk, T., Frangež, R., Svenson, J., 2019. Natural cholinesterase inhibitors from marine organisms. *Nat. Prod. Rep.* 36, 1053–1092.
- Nair, J.J., van Staden, J., 2013a. Pharmacological and toxicological insight to the South Africa Amaryllidaceae. *Food. Chem. Toxicol* 62, 262–275.

- Nair, J.J., Bastida, J., Codina, C., Viladomat, F., van Staden, J., 2013b. Alkaloids of the South African Amaryllidaceae: a review. *Nat. Prod. Commun* 8, 1335–1350.
- Nakanishi, K., Solomon, P.H., 1977. *Infrared Absorption Spectroscopy*. Holden Day, Oakland, pp. 17–44.
- Ogbole, O.O., Akinleye, T.E., Segun, P.A., Faleye, T.C., Adeniji, A.J., 2018. In vitro antiviral activity of twenty-seven medicinal plant extracts from Southwest Nigeria against three serotypes of echoviruses. *Virology* 15, 110.
- Ortiz, J.E., Garro, A., Pigni, N.B., Agüero, M.B., Roitman, G., Slanis, A., Enriz, R.D., Feresin, G.E., Bastida, J., Tapia, A., 2018. Cholinesterase-inhibitory effect and in silico analysis of alkaloids from bulbs of *Hieronymiella* species. *Phytomedicine* 39, 66–74.
- Pescitelli, G., Bruhn, T., 2016. Good computational practice in the assignment of absolute configurations by TDDFT calculations of ECD spectra. *Chirality* 28, 466–474.
- Pham, L.H., Döpke, W., Wagner, J., Mügge, C., 1998. Alkaloids from *Crinum amabile*. *Phytochemistry* 48, 371–376.
- Pretsch, E., Bühlmann, P., Affolter, C., 2000. *Structure Determination of Organic Compounds – Tables of Spectral Data*. Springer-Verlag, Berlin, pp. 161–243.
- Shaffer, R.D., 1972. *Synthetic and Biosynthetic Approaches to Cherylline and Related Compounds*. Unpublished Ph.D. Thesis, Library, Iowa State University of Science and Technology, Ames, USA.
- Superchi, S., Scafato, P., Górecki, M., Pescitelli, G., 2018. Absolute configuration determination by quantum mechanical calculation of chiroptical spectra: basics and applications to fungal metabolites. *Curr. Med. Chem.* 25, 287–320.
- Szelenyi, J., Bartha, E., Hollan, S., 1982. Acetylcholinesterase activity of lymphocytes: an enzyme characteristic of T-cells. *Br. J. Haematol.* 50, 241–245.

- Viladomat, F., Codina, C., Bastida, J., Mathee, S., Campbell, W.E., 1995. Further alkaloids from *Brunsvigia josephinae*. *Phytochemistry* 40, 961–965.
- Wagner, J., Pham, H.L., Döpke, W., 1996. Alkaloids from *Hippeastrum equestre* herb. -5. Circular dichroism studies. *Tetrahedron* 52, 6591–6600.

**Table 1**  
 $^1\text{H}$ ,  $^{13}\text{C}$  NMR and HMBC data of gigantelline and gigantellinine (1 and 2)<sup>a,b</sup>.

1				2		
No.	$\delta_{\text{C}}^{\text{c}}$	$\delta_{\text{H}}$	HMBC	$\delta_{\text{C}}^{\text{c}}$	$\delta_{\text{H}}$	HMBC
1	54.9 t	3.81 d (14.3)		58.9 t	3.72 br d (14.5)	N-Me, H <sub>2</sub> -3, H-8
		3.53 d (14.3)			3.47 br d (14.5)	
3	61.8 t	3.08 br dd (11.6, 5.9)	H-4, N-Me	63.4 t	3.06 br dd (11.6, 6.1)	H-4, H <sub>2</sub> -1, N-Me
		2.44 dd (11.6, 10.7) <sup>d</sup>			2.44 dd (11.6, 10.1) <sup>d</sup>	
4	44.3 d	4.18 dd (10.7, 5.9)	H-8, H-3',5'	45.9 d	4.13 dd (10.1, 6.1)	H-2', H-6', H <sub>2</sub> -3, H-5
4a	129.5 s		H-4, H-5, H-3A	129.5 s		H-8, H <sub>2</sub> -3
5	109.2 d	6.76 s	H-8, MeO-C6, H-2',6'	113.2 d	6.36 s	H <sub>2</sub> -1
6	147.9 s		H-5, MeO-C6	148.2 s		MeO-C6, H-8
7	147.8 s		H-8, MeO-C7	146.4 s		MeO-C6, H-5
8	112.0 d	6.37 s	H-5, H-4, MeO-C7	113.6 d	6.56 s	H-5, H <sub>2</sub> -1
8a	126.7 s		H-8, H <sub>2</sub> -1	128.2 s		H-5, H-4, H <sub>2</sub> -1
1'	134.5 s		H-2',6', H-3',5'	138.6 s		H-3', H-4
2'	129.6 d <sup>e</sup>	6.73 d (8.5) <sup>e</sup>	H-4, H-3',5'	121.5 d	6.67 dd (8.2, 2.1)	H-6'
3'	114.9 d <sup>f</sup>	7.00 d (8.5) <sup>f</sup>	H-2',6'	112.9 d	6.88 d (8.2)	
4'	155.9 s		H-2',6'	147.7 s		H-3', H-6', MeO-C4'
5'	114.9 d <sup>f</sup>	7.00 d (8.5) <sup>f</sup>	H-2',6'	148.1 s		H-3'
6'	129.6 d <sup>e</sup>	6.73 d (8.5) <sup>e</sup>	H-4, H-3',5'	117.1 d	6.60 d (2.1)	H-2', H-4
MeO-C6	57.4 q	3.83 s	H-5	56.4 q	3.62 s	
MeO-C7	55.1 q	3.59 s				
MeO-C4'				56.6 q	3.85 s	
N-Me	44.4 q	2.44 s <sup>d</sup>		46.0 q	2.43 s <sup>d</sup>	H-1B

<sup>a</sup> 2D  $^1\text{H}$ ,  $^1\text{H}$  (COSY) and  $^{13}\text{C}$ ,  $^1\text{H}$  (HSQC) NMR experiments confirmed the correlations of all the protons and the corresponding carbons.

<sup>b</sup> Coupling constants ( $J$ ) are given in parenthesis.

<sup>c</sup> Multiplicities were assigned with DEPT.

<sup>d</sup> These two signals are in part overlapped.

<sup>e</sup> These protons are magnetically equivalent.

<sup>f</sup> These protons are magnetically equivalent.

**Table 2**  
<sup>1</sup>H, <sup>13</sup>C NMR and HMBC data of gigancrine (3).<sup>a, b</sup>

No.	δ <sub>C</sub> <sup>c</sup>	δ <sub>H</sub> ( <i>J</i> in Hz)	HMBC
1	69.2 d	4.47 br s	H-3
2	54.9 d	3.12 d (3.8)	H-1, H-4A
3	53.5 d	3.48 m <sup>d</sup>	H-1, H <sub>2</sub> -4
4	24.9 t	2.37 ddd (15.4, 6.6, 2.4) 1.81 ddd (15.4, 11.0, 1.5)	H-4a
4a	60.6 d	3.21 dd (11.0, 6.6)	H <sub>2</sub> -4, H <sub>2</sub> -11
6	59.7 t	4.36 d (16.0) 3.89 d (16.0)	H-7, H-4a, H <sub>2</sub> -12
6a	122.6 s		H-10, H <sub>2</sub> -6
7	105.4 d	6.53 s	H-10, H <sub>2</sub> -6
8	146.6 s		H-10, H-7, H <sub>2</sub> -6
9	147.2 s		H-10, H-7
10	104.9 d	7.27 s	H-7
10a	138.2 s		H-10, H-7, H <sub>2</sub> -6
10b	47.0 s		H-10, H-2, H-1, H-4A, H <sub>2</sub> -11
11	34.9 t	2.27 ddd (13.0, 10.3, 8.2) 2.08 ddd (13.0, 8.2, 2.6)	H <sub>2</sub> -12, H-4a
12	48.2 t	3.48 m <sup>d</sup> 2.91 dt (12.8, 8.2)	H <sub>2</sub> -6, H-4a, H <sub>2</sub> -11
OCH <sub>2</sub> O	100.9 t	5.92 s (2H)	

<sup>a</sup> 2D <sup>1</sup>H, <sup>1</sup>H (COSY) and <sup>13</sup>C, <sup>1</sup>H (HSQC) NMR experiments confirmed the correlations of all the protons and the corresponding carbons.

<sup>b</sup> Coupling constants (*J*) are given in parenthesis.

<sup>c</sup> Multiplicities were assigned with DEPT.

<sup>d</sup> These two signals are overlapped.

**Table 3**  
**Comparison between experimental and calculated NMR data of gigancrinine (3).**

Experimental <sup>13</sup> C No.	$\delta_C$ (ppm)	Calculated <sup>a</sup> (1R,2R,3R)	(1S,2R,3R)	(1R,2S,3S)	(1S,2S,3S)
1	69.2	73	65.8	65.5	71.8
2	54.9	55.1	54.7	56	57.4
3	53.5	53	56.7	50.1	53.4
4	24.9	26.7	26.7	26.8	26.2
4a	60.6	61.3	59.5	60.4	65.6
6	59.7	61	60.9	60.9	61.1
6a	122.6	126.1	126.6	129.1	125.6
7	105.4	106.2	106	108.6	105.8
8	146.6	145.9	145.4	145.7	145.8
9	147.2	146.3	145.5	146.7	146.3
10	104.9	107	109.8	102.8	107.7
10a	138.2	139.2	135.7	137.5	140.2
10b	47.0	46.5	47.7	49.1	48.5
11	34.9	36.3	39.9	37.9	36.7
12	48.2	50.1	49.9	50.9	51
OCH <sub>2</sub> O	100.9	103.5	103.6	104	103.6
RMSD (ppm) <sup>b</sup>		1.8	2.7	2.7	2.3
Experimental <sup>3</sup> J <sub>HH</sub> Protons	J (Hz)	Calculated <sup>c</sup> (1R,2R,3R)	(1S,2R,3R)	(1R,2S,3S)	(1S,2S,3S)
H1-H2	n.d. <sup>d</sup>	0.0	5.6	2.3	3.3
H2-H3	3.8	3.1	3.5	3.7	3.7
H3-H4A	2.4	2.2	2.4	0.0	0.5
H3-H4B	1.5	1.8	1.9	6	6.1

<sup>a</sup> With the GIAO method at  $\omega$ B97X-D/6-31G(d) level, empirical corrections according to (Hehre et al., 2019).

<sup>b</sup> Root-mean-square deviation between experimental and calculated values.

<sup>c</sup> Fermi contact term calculated at  $\omega$ B97X-D/pcJ-0 level.

<sup>d</sup> Too small to be measured.

**Table 4****Anti-acetylcholinesterase activity of the alkaloids extracted from *C. jagus*, expressed in  $\mu\text{M}$ .**

Compound	IC <sub>50</sub> ( $\mu\text{M}$ ) <sup>a</sup>
Gigantelline (1)	n.s.
Gigantellinine (2)	174.90 $\pm$ 2.30
Gigancrinine (3)	n.s.
Sanguinine (4)	1.83 $\pm$ 0.01
Cherylline (5)	154.70 $\pm$ 1.01
Lycorine (6)	n.s.
Crinine (7)	161.30 $\pm$ 0.80
Flexinine (8)	164.60 $\pm$ 1.12
Hippadine (9)	n.d.
Galanthamine <sup>b</sup>	7.50 $\pm$ 0.02

<sup>a</sup> Not significant (n.s.) when the IC<sub>50</sub> was not reached and not determined (n.d.) when the compound could not be assayed because of its polarity.

<sup>b</sup> It was used as hydrobromide.



## Figure Legend

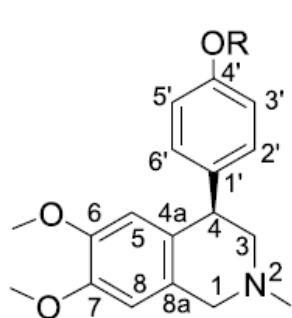
**Figure 1.** Structures of the isolated compounds (**1–9**).

**Figure 2.** The key correlations observed in the HMBC and NOESY spectra of alkaloids **1–3**.

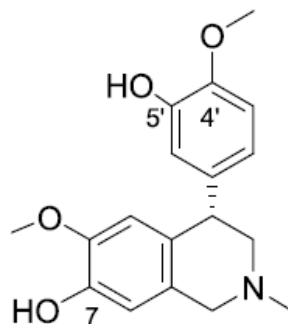
**Figure 3.** Experimental ECD spectra of gigantelline (**1**) (black solid line), gigantellinine (**2**) (blue dotted line) and cherylline (**5**) (green dashed line) measured in methanol (ca. 3 mM, 0.1 cm cell). (For interpretation of the references to color in this figure legend, the reader is referred to the Web version of this article.)

**Figure 4.** UV–vis absorption (top) and ECD spectra (bottom) of gigancrinine (**3**) measured in acetonitrile (solid lines, 8.0 mM, 0.01 cm cell) compared with spectra calculated for (1*R*,2*R*,3*R*,4*aR*,10*bS*)-**3** at the B3LYP/def2-TZVP/PCM level as Boltzmann average of 3 conformers at 300 K (dotted lines). Calculated spectra were obtained as sums of Gaussian bands with 0.25 eV exponential halfwidth, red-shifted by 5 nm, ECD spectrum scaled by a factor 3. (For interpretation of the references to color in this figure legend, the reader is referred to the Web version of this article.)

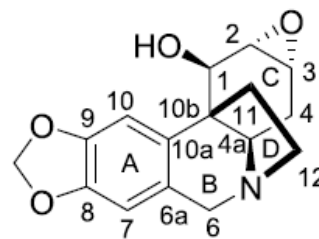
**Fig. 1. Structures of the isolated compounds (1–9).**



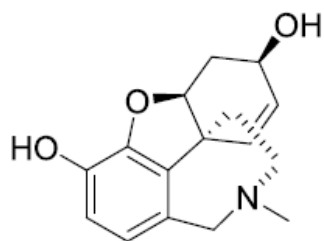
**1, Gigantelline, R=H**  
**10, 4'-O-Acetyl 1, R=Ac**



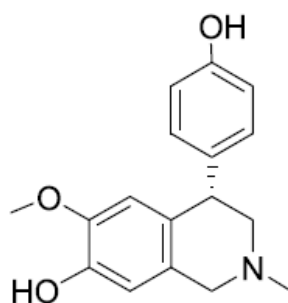
**2, Gigantellinine**



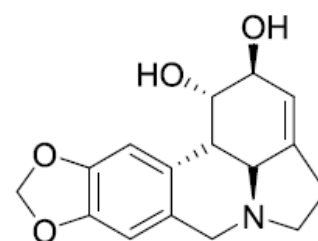
**3, Gigancrine**



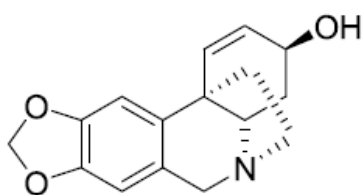
**4, Sanguinine**



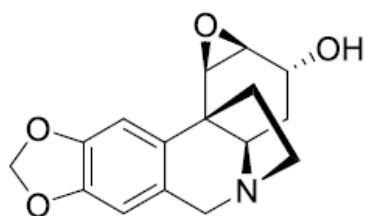
**5, Cherylline**



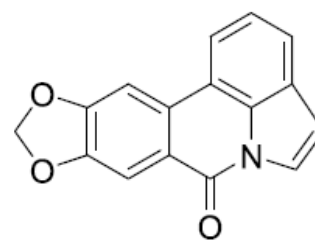
**6, Lycorine**



**7, Crinine**



**8, Flexinine**



**9, Hippadine**

**Fig. 2.** The key correlations observed in the HMBC and NOESY spectra of alkaloids 1–3.

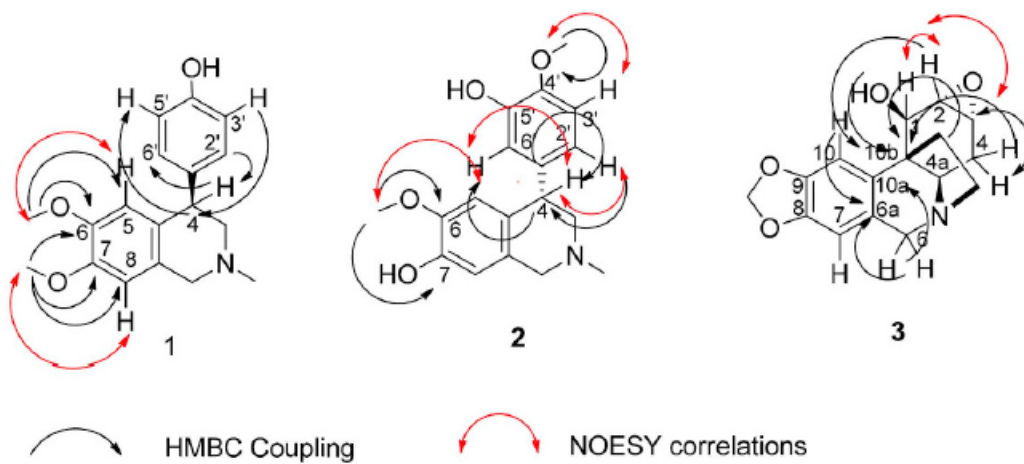


**Fig. 3.** Experimental ECD spectra of gigantelline (1) (black solid line), gigantellinine (2) (blue dotted line) and cherylline (5) (green dashed line) measured in methanol (ca. 3 mM, 0.1 cm cell). (For interpretation of the references to color in this figure legend, the reader is referred to the Web version of this article.)

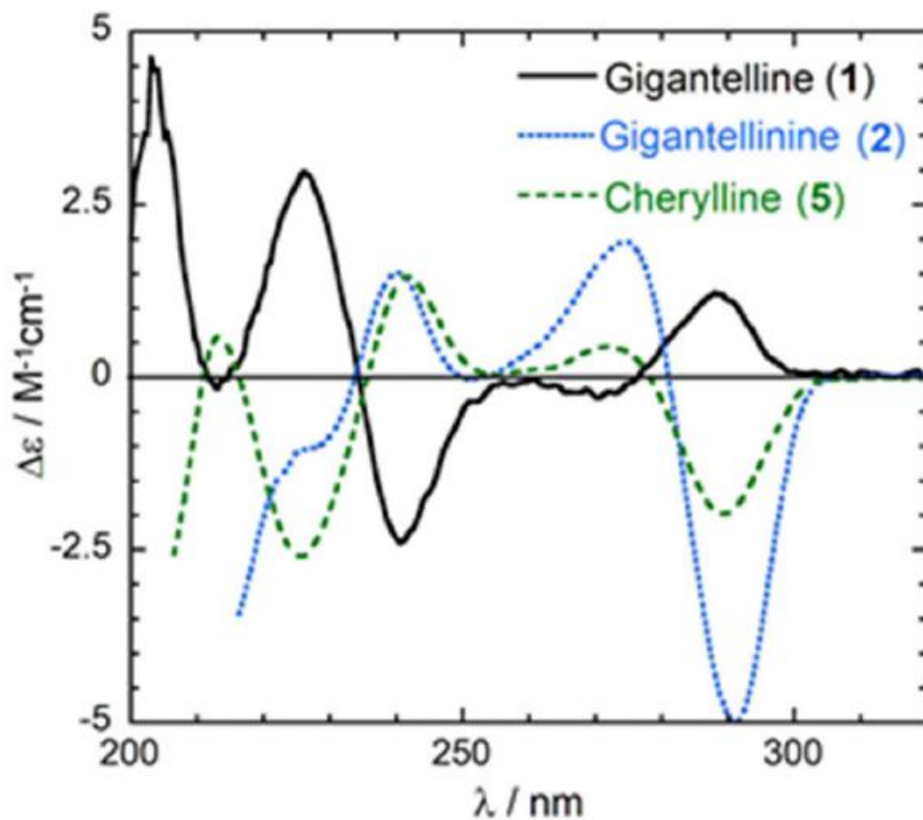


Fig. 4. UV–vis absorption (top) and ECD spectra (bottom) of gigancrine (3) measured in acetonitrile (solid lines, 8.0 mM, 0.01 cm cell) compared with spectra calculated for (1*R*,2*R*,3*R*,4*aR*,10*bS*)-3 at the B3LYP/def2-TZVP/PCM level as Boltzmann average of 3 conformers at 300 K (dotted lines). Calculated spectra were obtained as sums of Gaussian bands with 0.25 eV exponential halfwidth, red-shifted by 5 nm, ECD spectrum scaled by a factor 3. (For interpretation of the references to color in this figure legend, the reader is referred to the Web version of this article.)

